Published in final edited form as:
Nature. 2017 October 12; 550(7675): 270–274. doi:10.1038/nature24037.

Cancer Drug Addiction is Relayed by an ERK2-Dependent Phenotype Switch

Xiangjun Kong[1], **Thomas Kuilman**[1], **Aida Shahrabi**[1], **Julia Boshuizen**[1], **Kristel Kemper**[1], **Ji-Ying Song**[2], **Hans W.M. Niessen**[3], **Elisa A. Rozeman**[1], **Marnix H. Geukes Foppen**[1], **Christian U. Blank**[1], and **Daniel S. Peeper**[1,*]

[1]Division of Molecular Oncology and Immunology, The Netherlands Cancer Institute, Plesmanlaan 121, 1066 CX Amsterdam, The Netherlands [2]Division of Experimental Animal Pathology, The Netherlands Cancer Institute, Plesmanlaan 121, 1066 CX Amsterdam, The Netherlands [3]Department of Pathology and Cardiac Surgery, VU University Medical Center, ACS, 1007 MB Amsterdam, The Netherlands

Abstract

Drug addiction denotes the dependency of tumors on the same therapeutic drugs to which they have acquired resistance. Observations from cultured cells1–3, animal models4 and patients5–7 raise the possibility that cancer drug addiction can instigate a potential cancer vulnerability, which may be used therapeutically. However, for this trait to become of clinical interest, it is imperative to first define the underlying mechanism. Therefore, we performed an unbiased CRISPR-Cas9 knockout screen to functionally mine the genome of melanoma cells that are both resistant and addicted to BRAF inhibition for “addiction genes”. Here, we describe a signaling pathway comprising ERK2, JUNB and FRA1, disruption of which allows tumor cells to reverse addiction and survive upon treatment discontinuation. This occurred both in culture and mice, and was irrespective of the acquired drug resistance mechanism. In melanoma and lung cancer cells, death induced by drug withdrawal was preceded by a specific ERK2-dependent phenotype switch, alongside transcriptional reprogramming reminiscent of EMT. In melanoma, this caused shutdown of the lineage survival oncoprotein MITF, restoration of which reversed both phenotype switching and drug addiction-associated lethality. In melanoma patients who had progressed on BRAF inhibition, treatment cessation was followed by increased expression of the phenotype switch-associated receptor tyrosine kinase AXL. Drug discontinuation synergized with the melanoma

*Correspondence and requests for materials should be addressed to D.S.P. (d.peeper@nki.nl).

Author contributions

X.K., T.K. and D.S.P. designed all experiments. All *in vitro* experiments were carried out by X.K., with the exception of an RT-PCR analysis by K.K. Xenograft experiments were done by A.S. T.K. performed all bioinformatic analyses. J.-Y.S. analyzed mouse tumors, J.B., E.A.R., M.H.G.F. and H.W.M.N. analyzed human melanoma samples in collaboration with C.U.B.. X.K. and D.S.P. wrote the manuscript. All authors revised and approved the manuscript. The project was supervised by D.S.P.

The authors declare no competing financial interests.

Data availability

All sequencing datasets have been deposited in the NCBI Gene Expression Omnibus under accession number GSE98866 and GSE98867.

Europe PMC Funders Author Manuscripts

chemotherapeutic dacarbazine by further suppressing MITF and its prosurvival target BCL2 while inducing DNA damage. Our results uncover a pathway driving cancer drug addiction, which may guide alternating therapeutic strategies for enhanced clinical responses of drug-resistant cancers.

We treated a panel of $BRAF^{V600E}$ melanoma cell lines with either BRAF inhibitor dabrafenib or dabrafenib + MEK inhibitor trametinib. As expected, all four cell lines were highly sensitive to these drugs (Fig. 1a). After 3-5 months, pools of cells emerged that had apparently developed resistance to the lethal drug dose (labeled 'BR' for BRAF inhibitor-Resistant and 'BMR' for BRAF + MEK inhibitor-Resistant). Strikingly however, when drug treatment was acutely discontinued, these drug-resistant cells massively died (Fig. 1b and Extended Data Fig. 1); apparently, they had become addicted to the very drugs that served to eliminate them.

To functionally screen for essential drug addiction genes, a lentiviral CRISPR-Cas9 GeCKO library8 was introduced into drug-treated $451Lu^{BR}$ cells (Fig. 1c). Thirty days after drug withdrawal, 13 clones emerged, which apparently had lost the drug addiction phenotype. For nine of these, we identified sgRNAs in ≥2 individual clones (Fig. 1d, for full sequencing data, see Supplementary table 1) targeting genes encoding several factors known to communicate to one another, namely ERK2, JUNB and MEK1, while also FRA1 (a JUNB partner) was included for further analyses. A first validation round confirmed that the sgRNAs had caused the expected perturbations of genes encoding ERK2 (with intact ERK1; Fig. 1e), JUNB (Fig. 1f), MEK1 (Fig. 1g) and FRA1 (Fig. 1h). Thus, a genome-wide perturbation screen successfully identified a signaling pathway responsible for the drug addiction phenotype.

To determine the generality of these screen hits, we used a panel of melanoma cell lines that had acquired drug resistance through distinct mechanisms: $451Lu^{BR}$ showed hyperactivation of the ERK pathway (Extended Data Fig. 2a) while harboring an activating $MEK1^{K57N}$ mutation (Fig. 2a); MEK-ERK signaling was also boosted in $A375^{BMR}$ cells, which carry a *BRAF* amplification (Fig. 2b and Extended Data Fig. 2b, c); $Mel888^{BMR}$, too, show hyperactivated MEK-ERK signaling and harbor a kinase domain duplication (Fig. 2c and Extended Data Fig. 2d), which we have characterized recently9. $A101D^{BMR}$ cells, in contrast, acquired drug resistance without detectable ERK reactivation (Fig. 2d).

Whereas control melanoma cells died massively upon drug withdrawal, knocking out ERK2 resulted in a vigorous rescue, across the entire cell panel (Fig. 2e, f). In contrast, genetic perturbation of ERK1 failed to prevent lethal drug addiction. Similar to ERK2, genetic inactivation of JUNB generally rescued drug addiction-associated death (Fig. 2g, h), as did FRA1 loss (Fig. 2i, j). Knocking out MEK1, too, rescued drug addiction, but only in $451Lu^{BR}$ cells (Extended Data Fig. 3a, b). This was due to its resistance mechanism, a $MEK1^{K57N}$ activating mutation (Fig. 2a, 1g) rendering this cell line susceptible to breaking drug addiction upon MEK1 inactivation. Thus, ERK2, JUNB and FRA1 validated across a heterogeneous cell line panel, highlighting their common mechanism of action independent of how cells achieved therapy resistance.

Europe PMC Funders Author Manuscripts

To determine whether the drug addiction phenotype also manifests *in vivo*, we established melanoma xenografts in the presence of both dabrafenib and trametinib. When treatment was ceased, control tumors regressed, in contrast to JUNB- and ERK2- knockout tumors, which continued to expand (Fig. 2k), indicating that the drug addiction phenotype is also seen tumors.

These findings implicated ERK signaling in the sensitivity of drug-resistant cells to treatment discontinuation. In 451Lu^{BR}, A375^{BMR} and Mel888^{BMR} cells, we observed hyperactivation of MEK-ERK upon drug withdrawal, a so-called rebound signal (Extended Data Fig. 4a). Remarkably, also A101D^{BMR} cells, which are resistant to BRAF + MEK inhibition in an ERK-independent fashion (Fig. 2d), showed an equally intense ERK rebound upon drug washout. This result uncouples the mechanism of acquired drug resistance from the signaling manifesting drug addiction. Corroborating these findings, also a low dose of ERK inhibitor completely rescued lethality by drug withdrawal not only in the three cell lines with ERK rebound (consistent with Moriceau G et al.3) but also in A101D^{BMR} cells (Extended Data Fig. 4b). Thus, regardless of the resistance mechanism, melanoma cells commonly show ERK rebound upon drug withdrawal, which contributes to the drug addiction trait.

Given the identification of JUNB and FRA1 in our screen, two key signaling transcription factors, we investigated whether drug addiction is relayed by transcriptional reprogramming. RNA profiling of drug-addicted cells upon drug cessation revealed a common expression alteration in two cell lines for the top 200 variant genes (Extended Data Fig. 5a). This was accompanied by a major switch in the activity of genes involved in cell proliferation and those contributing to cell invasion, reminiscent of changes seen for “phenotype switching”: transcriptional and phenotypic plasticity between alternative proliferative and invasive states10–12 (Fig. 3a).

MITF is a pivotal transcription factor driving the specification and survival of the melanocytic lineage13 and plays a central role in melanoma phenotype switching11. Consistently, gene set enrichment analysis (GSEA) revealed a strong negative association between the drug withdrawal and an MITF signature (Fig. 3b), with many MITF targets being strongly downregulated upon drug withdrawal. GSEA confirmed that AP-1, TEAD and JUNB transcriptional signatures14 were enriched upon drug withdrawal (Extended Data Fig. 5b), further supporting the notion that cells underwent phenotype switching.

Concordantly, MITF protein levels declined upon drug withdrawal, in all four cell lines examined (Fig. 3c). As a result, both MITF-controlled Melan-A and prosurvival BCL2 proteins were downregulated. Conversely, drug withdrawal was associated with the upregulation of fibronectin and downregulation of E-cadherin, two EMT proteins. We and others previously reported that MITF expression is inversely correlated with that of the receptor tyrosine kinase AXL15,16. Consistent with this, AXL was induced by drug removal, as were JUNB and FRA1 (Fig. 3c). cJUN can mediate a melanoma phenotype switch upon BRAF inhibition and cytokine treatment17,18, but was not strongly nor consistently induced (Fig. 3c) while its ablation failed to prevent cell death induced by drug withdrawal (Extended Data Fig. 5c, d). Upon drug withdrawal, cells became highly

migratory, another key feature of EMT (Extended Data Fig. 5e, f). Furthermore, the phenotype switch was not seen in non-drug-addicted cells (Extended Data Fig. 6a, b).

To investigate whether this can be recapitulated in a clinical setting, we performed immunohistochemical analysis on a set of tumor biopsies from BRAF inhibitor-relapsed melanoma patients. This cohort comprised tumors both from patients who were still on BRAFi treatment at the time of the biopsy and patients who were already taken off the drug. We observed that in a highly significant number of cases, treatment discontinuation correlated with increased expression levels of AXL (Fig. 3d), indicating that at least some features of EMT/phenotype switching are also observed in patients.

To examine any contribution of MITF to the phenotype switch, we restored its expression prior to drug withdrawal (Fig. 3e). MITF was at least partially functional, as judged by the attenuation of Melan-A downregulation. Its restoration led to substantial protection to death by drug withdrawal (Fig. 3f), demonstrating that drug addiction is accompanied by an MITF-dependent phenotype switch, which underlies the associated loss of fitness.

To determine whether the screen hits were functionally connected to phenotype switching, we generated ERK2 and JUNB knockout pools and performed RNA sequencing upon drug withdrawal. A shift in transcriptional patterns occurred in control cells upon drug removal, but this was diminished in the ERK2 knockout derivatives and to a somewhat lesser extent in the JUNB knockout cells (Extended Data Fig. 7a). Consistently, the phenotype switch upon drug withdrawal was reverted in the absence of either ERK2 or JUNB proteins (Extended Data Fig. 7b). Rescue of drug washout-induced cell death by ERK2 or JUNB depletion was strongly correlated with maintenance of the MITF signature, and a lack of AP-1, TEAD and JUNB-associated genes (Extended Data Fig. 7c). As a consequence, the phenotypic changes in cell morphology upon drug withdrawal were neutralized in the ERK2 and JUNB knockout cell lines, but not in ERK1 knockout cells (Fig. 3g).

To determine whether ERK2 is a master regulator of the phenotype switch as a function of drug addiction, we analyzed the expression levels of several proteins associated with this switch. This result was highly informative: first, upon loss of ERK2, MITF and its downstream targets BCL2 and Melan-A were no longer downregulated after drug removal (Fig. 3h). Second, the induction of JUNB and FRA1 upon drug withdrawal was diminished in ERK2 knockout cells (but not in ERK1 knockout cells). Third, also ablation of JUNB prevented the decline in MITF after drug withdrawal; it did however not affect ERK levels nor activity, suggesting that JUNB acts downstream of ERK and upstream of MITF. Fourth, cells lacking either ERK2 or JUNB, but again not ERK1, failed to undergo the EMT-like changes upon drug withdrawal, as judged by fibronectin and E-cadherin expression. In addition to genetic inactivation, also pharmacologic inhibition of ERK neutralized both changes in gene expression (Extended Data Fig. 8a) and morphology (Extended Data Fig. 8b) upon drug withdrawal.

These *in vitro* observations were corroborated *in vivo*: whereas upon drug discontinuation, established $A375^{BMR}$ tumors (Fig. 2k) were largely negative for MITF and its targets Melan-A and GP100, in contrast JUNB or ERK2 knockout melanomas retained expression

of MITF and its targets (Fig. 3i). These results demonstrate that ERK2 and JUNB act in an MITF-dependent genetic phenotype switching program governing drug addiction.

Increasing the levels and phosphorylation of ERK1 to those seen for ERK2 upon drug removal failed to cause cell death in the absence of ERK2, suggesting that ERK2 functions distinctly from ERK1 in the context of drug addiction (Extended Data Fig. 9a, b), consistent with their different activities in EMT19. Furthermore, in addition to acquired resistance, also upon on enforced BRAFi resistance (by ectopic expression of mutant MEK1^{T55delinsRT} 20), tumor cell viability declined upon drug withdrawal, as well as levels of MITF and its targets (Extended Data Fig. 8c, d).

Since acquired resistance to precision drugs is commonly seen across tumor types and drugs, we investigated whether the ERK2/JUNB-dependent drug addiction mechanism is operational in lung cancer, too. Upon drug withdrawal, EGFR inhibitor CL-387,785-refractory and -addicted1 HCC827 cells showed loss of fitness (Fig. 4a). Similarly to melanoma, pharmacologic (Extended Data Fig. 8e) or genetic ablation of ERK2 (but not ERK1) rescued the drug addiction of these NSCLC cells (Fig. 4a, b). Loss of fitness by drug withdrawal was preceded by several events also seen for melanoma cells, including hyperactivation of ERK and MEK and an EMT/phenotype switch (Fig. 4c). We conclude that the specific ERK2-JUNB-FRA1 pathway responsible for drug addiction is not limited to one particular tumor / treatment setting.

Although the extent of lethality imposed by drug addiction can be near-total (Fig. 1b, explaining the very low background in our screen), in the long run drug withdrawal-resistant clones spontaneously arose in cell pools (Extended Data Fig. 10a). Functional and biochemical analysis (Extended Data Fig. 10b, c) revealed that these drug withdrawal-resistant clones had regained responsiveness to MAPK pathway inhibition. This is in line with successful clinical rechallenges with MAPK inhibitors in patients who had progressed on treatment21,22.

In a patient setting, emergence of drug withdrawal-resistant cells could be detrimental and prevent a durable clinical response. Therefore, we considered combining the cessation of BRAF inhibition with the initiation of another treatment. The chemotherapeutic dacarbazine (brand name DTIC) is an anticancer alkylating agent, which in the last decade has been commonly used as a single agent for metastatic melanoma, albeit with poor response rates23. We sought to find a therapeutic window to determine whether dacarbazine acts cooperatively with a discontinuation of treatment for the first treatment (BRAF inhibition), creating an alternating therapy. Increasing dacarbazine concentrations to up to 500 μg/ml had little cytotoxic effect on two drug-resistant and moderately drug-addicted melanoma cell lines in the presence of BRAF inhibitor (Fig. 4d). In contrast, there was a strong synergy when dacarbazine was administered upon withdrawal of BRAF inhibitor. This was accompanied by a synergistic induction of γH2AX, a marker of double strand DNA damage (Fig. 4e). Furthermore, this cooperatively suppressed MITF and its targets Melan-A and BCL2 (Fig. 4e). The reduction of the latter prosurvival protein, alongside the induction of DNA damage, provides a plausible mechanistic explanation for the observed synergy in induction of cell death between drug withdrawal and dacarbazine.

It has been proposed that alternating or intermittent therapeutic strategies may create larger therapeutic windows21,24–26. Since we observe that after a long drug holiday, rare resistant clones can emerge, we propose that rather than a plain drug holiday one ought to explore optimal alternating treatment modalities. Our results suggest that insight into the molecular mechanism of drug addiction (which seems to be conserved among different tumor types and targeted agents) may guide rational alternating treatment strategies to enhance the extent of killing of drug-resistant cells and allow for more durable clinical benefit.

Methods

Genome-wide CRISPR-cas9 knockout (GeCKO) screen

Drug-addicted 451Lu^{BR} cells were lentivirally transduced with two GeCKO libraries (A and B)8. Two days after infection, cells were selected with puromycin (2 μg/ml) for 3 days. Cells were split into two pools, and one arm was subjected to BRAFi dabrafenib (1 μM) treatment, whereas the other arm was left untreated. Colonies formed in the drug-deprived group were individually picked and expanded. For identification of sgRNAs in individual clones, genomic DNA was isolated and sgRNAs were recovered by PCR amplification. Amplified DNA fragments were cloned into the TOPO TA-cloning vector (450071, Invitrogen) followed by identification of the sgRNA by Sanger sequencing.

Compounds

BRAF inhibitors dabrafenib and PLX4720, MEK inhibitor trametinib, ERK inhibitor SCH772984 and EGFR tyrosine kinase inhibitor CL-387,785 were purchased from Selleck Chemicals (Houston, TX, USA). Dacarbazine was obtained from the pharmacy of the Slotervaart hospital (Amsterdam, The Netherlands).

Cell lines

A375, Mel888, A101D, SK-Mel-28, D10 and HEK293T cells were from the Peeper laboratory cell line stock. HCC827 and HCC827^{CLR} cells were from K. Suda and T. Mitsudomi (Kindai University) and 451Lu cells from J. Villanueva (The Wistar Institute). All cell lines were authenticated by STR profiling (Promega) and routinely tested for mycoplasma contamination. All cell lines were cultured in DMEM supplemented with 9% fetal bovine serum (Sigma), plus 100 units per ml penicillin and 0.1 mg ml–1 streptomycin (Gibco). To generate BRAFi or BRAFi + MEKi-resistant cells, parental drug-sensitive cells were exposed to increasing concentrations of BRAFi dabrafenib (from 0.01 μM to 5 μM) or BRAFi dabrafenib + MEKi trametinib (from 0.01 μM + 0.001 μM to 0.5 μM + 0.05 μM) for 3–5 months. PLX4720-resistant cells were generated as previously described16. The resistance was confirmed by measuring cell viability under drug treatment.

Colony formation assay

Colony formation assays were performed in 12 well plates by seeding 3,000 cells (A101D^{BMR}), 10,000 cells (HCC827^{CLR} and all parental drug-sensitive cells), 30,000 cells (Mel888^{BMR}), or 50,000 cells (451Lu^{BR}, A375^{BMR}, A375^{BR} and D10^{BR}). Medium was refreshed twice per week and plates were fixed in 4% formaldehyde solution, stained with

crystal violet (1% in 50% methanol) and photographed after 10-21 days of treatment (as indicated).

Animal studies

Animal work procedures were approved by the animal experimental committee of the NKI and performed according to Dutch law. The *in vivo* experiment was performed with $A375^{BMR}$ cells infected with lentivirus encoding sgRNAs. 10^6 cells were s.c. injected into the both flanks of 5-7-week-old female NSG mice. The mice received dabrafenib and trametinib by daily oral gavage from the first day of tumor injection onwards until drug treatment was stopped. Tumor growth rates were analyzed by measuring tumor length (L) and width (W), and calculating volume through the use of the formula $LW^2/2$. Mice were not randomized for the experiment. Investigators were not blinded when assessing the outcome of the experiment.

Human melanoma specimens

Patient melanoma samples were obtained (following Institutional Review Board approval) from the NKI-AVL pathology archive biobank. Informed consent was obtained from all patients.

Immunohistochemistry and scoring

AXL staining was performed manually using the following protocol: after deparaffinization of FFPE fixed slides using xylene, antigen retrieval was performed using citrate buffer (pH 6) in a pressure cooker for 5 minutes. Sections were treated with 0.3% H_2O_2 to block endogenous peroxidase activity and subsequently blocked in 10% human serum in PBS-T for 30 minutes. Primary AXL antibody (sc-20471, Santa Cruz) was applied at a concentration of 3 μg/ml for 1 hour at room temperature. Detection was performed by an anti-rabbit HRP conjugated antibody (Immunologic, Brightvision) and developed using AEC and a counterstain of hematoxylin. Slides were manually analyzed by a certified pathologist from the VU medical Center (Amsterdam, The Netherlands) in a blinded fashion. Percentage AXL positive cells was determined by analyzing whole slides of every sample. MITF (clone C5/D5, Immunologic) and Melan-A and GP100 (ab732, Abcam) stainings in mouse xenograft tumors were performed with the protocol described above with minor modifications (block with goat serum and develop with DAB).

Immunoblotting

Immunoblotting was performed as previously described16. The following antibodies were used: pERK1/2 (Thr202/Tyr204, 9106), ERK1/2 (9102), pMEK1/2 (Ser217/221, 9154), MEK1/2 (4694), MEK1 (2352), MEK2 (9147), JUNB (3753), pFRA1 (Ser265, 5841), p-cJUN (Ser73, 3270) and cJUN (2315) BCL2 (4223) from Cell Signaling Technology; $BRAF^{V600E}$ (E19290) from Spring Bioscience; ATK (sc-8312), pAKT (Ser473, sc-7985-R), FRA1 (sc-28310), BRAF (sc-5284), BCL2 (sc-492) and HSP90 (sc-7947) from Santa Cruz Biotechnology; MITF (ab12039) and AXL (ab89224) from Abcam; Melan-A (M7196) from Dako; E-Cadherin (610181), Vimentin (550513) and Fibronectin (610077) from BD Bioscience.

Europe PMC Funders Author Manuscripts

Fluorescence In Situ Hybridization

Preparation of metaphase chromosome spreads from A375 and A375^{BMR} cells was performed as described previously27. Two-color metaphase FISH was performed using a BRAF probe (7q34 BRAF-CN RD, G100368R-8, Agilent) and a probe located on the chromosome 7 centromere (Chr7 CEP GR, G100527G-8, Agilent) according to the manufacturer's protocol.

PCR, Sanger sequencing, cloning and lentivirus production

All primer sequences are listed in Supplementary table 2. For identification of BRAF amplification in A375^{BMR} cell, genomic DNA was isolated and quantitative PCR was performed with primers amplifying BRAF, CRAF and LINE. For identification of the MEK1 mutation in 451Lu^{BR} cells, genomic DNA was isolated and MEK1 exon 2 was cloned into the TOPO TA-cloning vector (450071, Invitrogen), which was followed by Sanger sequencing. The presence of BRAF$^{V600E/DK}$ in Mel888^{BMR} cell was identified as previously described9. Cloning of sgRNAs into LentiCRISPRv2 vector was performed as described (http://www.genome-engineering.org/crispr/). Briefly, the LentiCRISPRv2 plasmid was digested with *BsmB*I and gel-purified. DNA oligonucleotides (Invitrogen) were annealed and ligated into the digested vector. Target sgRNA oligonucleotide sequences are listed in Supplementary table 2. The plasmid encoding the MITF-M isoform was previously described16. Production of lentivirus was performed as described previously28.

Transwell Migration assay

To examine the migration potential, cells were cultured in the presence or absence of MAPKi for 1 day followed by seeding 200,000 cells in the top chambers of a transwell (3422, Corning) in serum-free medium with or without inhibitors. The lower compartment contained medium supplemented with 9% fetal bovine serum as a chemoattractant. Cells were incubated for 8 (A101D^{BMR}) or 24 (451Lu^{BR}) hours and cells that did not migrate through the pores were removed by a cotton swab. Filters were fixed in 4% formaldehyde solution, stained with 0.1% crystal violet, photographed and cells numbers were counted.

RNA sequencing analysis

RNA was isolated using Trizol, and cDNA libraries were sequenced on an Illumina HiSeq2000 to obtain 65 bp single-end sequence reads. Reads were aligned to the GRCh38 human reference genome using Tophat (2.1.0), and gene counts were obtained using HTSeq-count. All downstream analyses were performed in R using the Bioconductor framework. DESeq2 rlog-values were used for visualization of gene expression levels in heat maps. Heat maps represent mean rlog-values of two independent biological replicate experiments. Clustering was performed using default settings of the heatmap.2 function in the gplots package. For Extended Data Fig. 5a, gene-wise scaling was applied to rlog-values, and the 200 most variable are represented. For Fig. 3a and Extended Data Fig. 7a, b, rlog-values were mean normalized on a gene-wise basis. For gene set enrichment analyses, counts per million (cpm) were used as input. For Fig. 3b and Extended Data Fig. 5b, time points were converted to a ranking score (0, 1, 2 or 3 for time points 0, 6, 24 or 48 h of A375^{BMR} and 0, 1, 3 or 5 days of 451Lu^{BR}, respectively); for Extended Data Fig. 7c, the extent of rescue

from cell death was converted to a ranking score (1, 2, 3, or 4 for Mel888^{BMR} cells expressing sgCtrl, sgJUNB, or sgERK2 in the context of drug removal, and Mel888^{BMR} cells with treatment, respectively). Pre-ranked gene lists were created by correlating these ranking scores with gene expression using the Spearman's rank correlation coefficient metric. Phenotype switching and MITF target gene lists were obtained from http://www.jurmo.ch/work_mitf.php. The TEAD and AP1 signatures were taken from Verfaillie et al.14, and the JUNB signature was derived from supplemental table 3A of Fontana et al.29, where human homologs of mouse genes were derived using the biomaRt package. Analyses were performed using javaGSEA30, and replotted from the output of this tool using the replotGSEA function (https://github.com/PeeperLab/Rtoolbox).

Extended Data

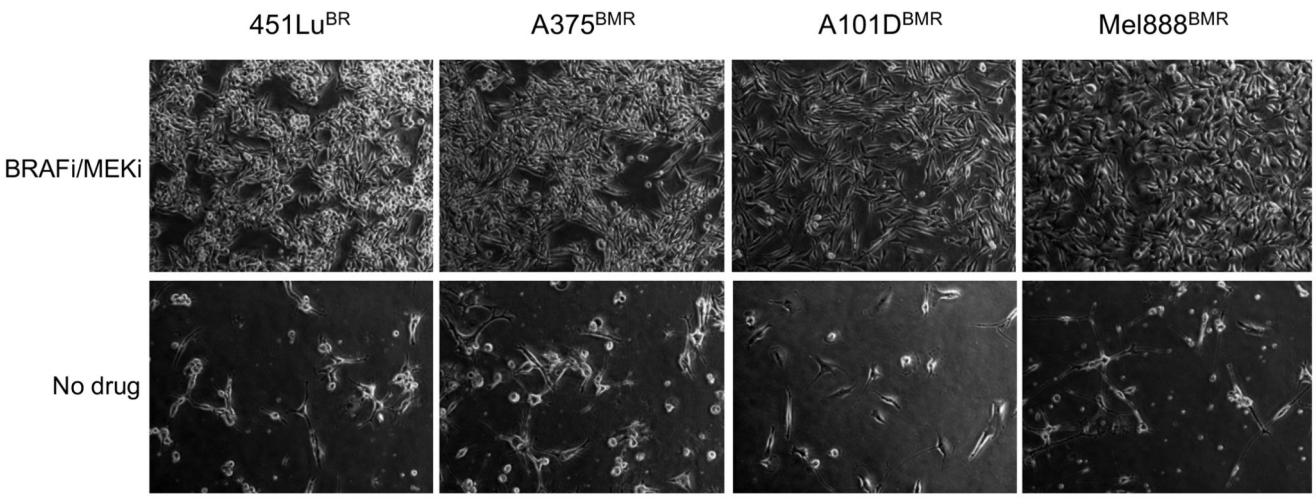

Extended Data Figure 1. Drug addiction phenotype in acquired drug resistance melanoma cells

Acquired BRAFi resistant 451Lu^{BR} cell were cultured in the presence or absence of 1 μM BRAFi; acquired BRAFi + MEKi resistant A375^{BMR}, A101D^{BMR} and Mel888^{BMR} cells were cultured in the presence or absence of 0.5 μM BRAFi + 0.05 μM MEKi. Photographs were taken after 7 days. The images shown here are representative of three independent biological experiments.

Europe PMC Funders Author Manuscripts

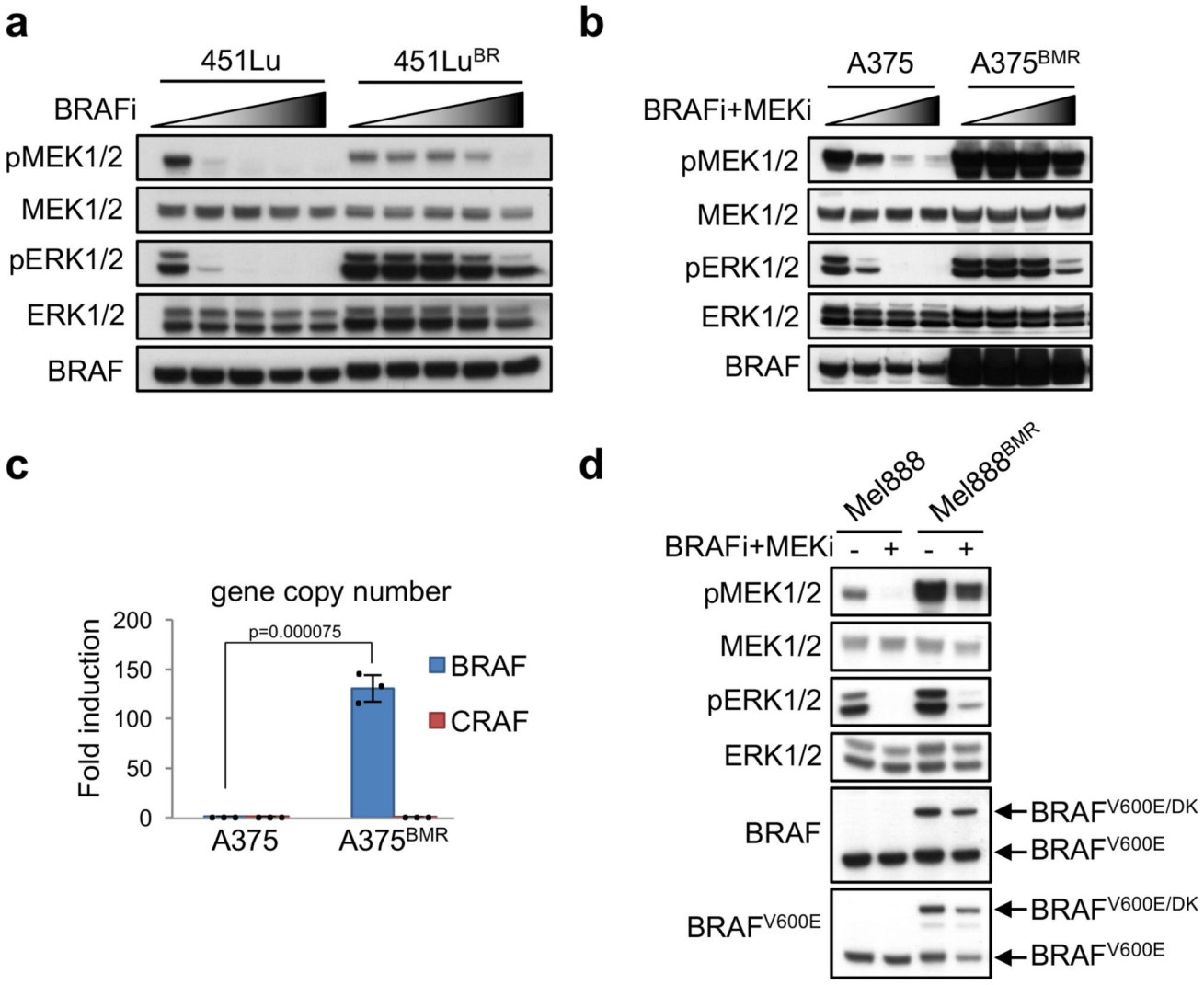

Extended Data Figure 2. Generation of a diverse melanoma cell line panel with distinct drug resistance mechanisms

(**a**) 451Lu and 451Lu^{BR} cells were treated with increasing concentrations of the BRAFi dabrafenib (0, 0.01, 0.1, 1 and 10 μM) for 6 hours. Total cell lysates were subjected to immunoblotting with indicated antibodies. ERK1/2 served as a loading control.

(**b**) A375 and A375^{BMR} cells were treated with increasing concentrations of the BRAFi dabrafenib + MEKi trametinib (0 + 0, 0.01 + 0.001, 0.1 + 0.01 and 1 + 0.1 μM) for 6 hours. Total cell lysates were subjected to immunoblotting with indicated antibodies. ERK1/2 served as a loading control.

(**c**) Quantification of *BRAF* amplification by qPCR on genomic DNA of A375 and A375^{BMR} cells. *CRAF* was included as a negative control. CT values were normalized to *LINE*. P-value calculated by unpaired two-sided Student's t-test; Data in graphs are mean ± s.d. from three technical replicates; Confidence interval 95%.

Europe PMC Funders Author Manuscripts

(**d**) Mel888 and Mel888^{BMR} cells were treated with vehicle or 0.5 μM BRAFi + 0.05 μM MEKi for 6 hours. Total cell lysates were subjected to immunoblotting with indicated antibodies. ERK1/2 served as a loading control.

For gel source images, see Supplementary Fig. 1. Data in **a**-**d** are representative of three independent biological experiments.

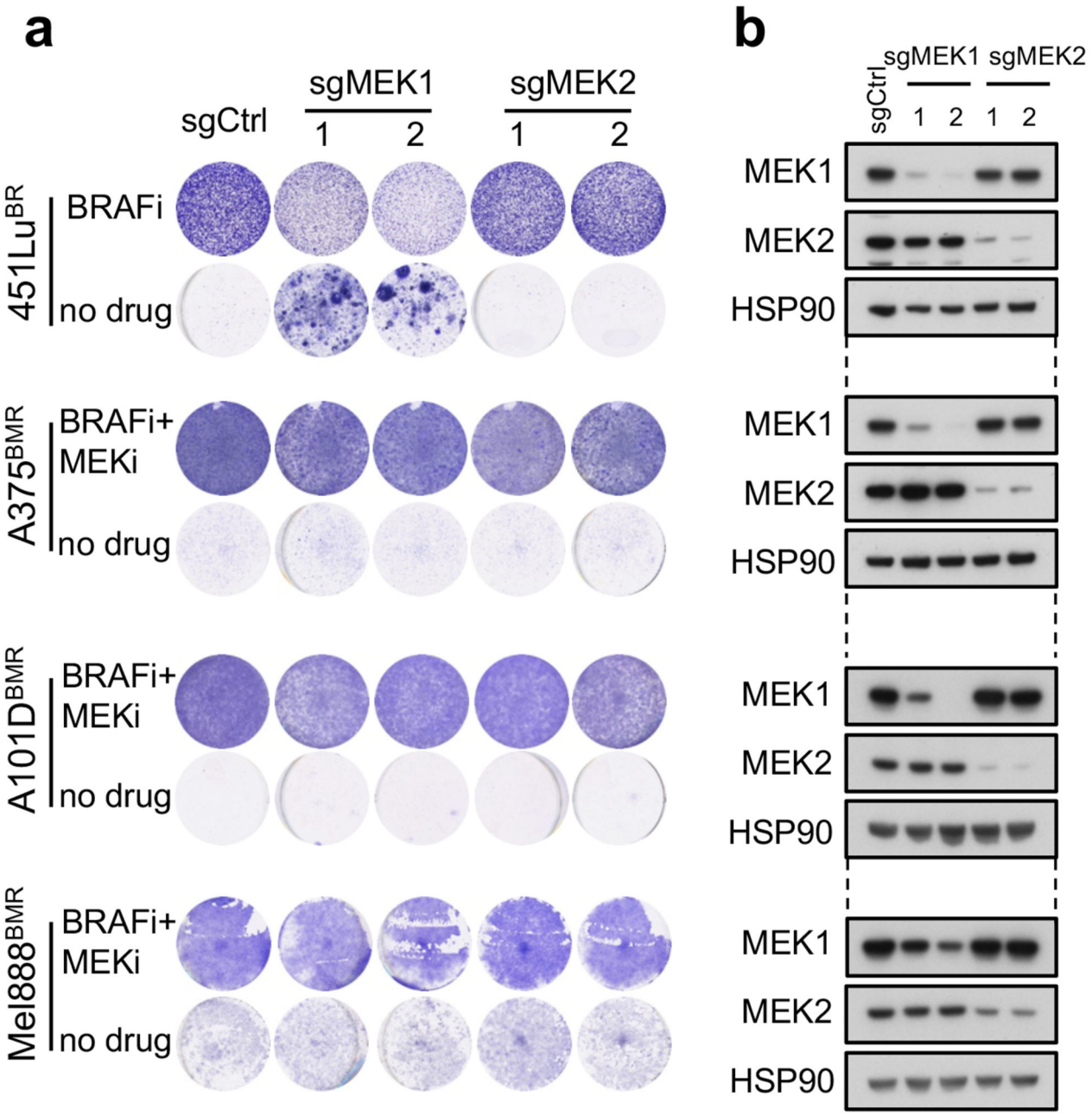

Extended Data Figure 3. Disruption of MEK1 rescues drug addiction phenotype in 451Lu^{BR} cell

Europe PMC Funders Author Manuscripts

(**a**) 451Lu^{BR}, A375^{BMR}, A101D^{BMR} and Mel888^{BMR} cells were infected with lentivirus expressing sgRNAs targeting either genes encoding MEK1 (sgMEK1), MEK2 (sgMEK2) or a scrambled sequence (sgCtrl). Cells were seeded in the presence or absence of MAPK inhibitors, and fixed, stained and photographed after 14 days (BRAFi or BRAFi + MEKi group) or 21 days (no drug group).

(**b**) Cell lysates from (**a**) were subjected to immunoblotting using the indicated antibodies. HSP90 served as a loading control.

For gel source images, see Supplementary Fig. 1. Data in **a** and **b** are representative of three independent biological experiments.

Europe PMC Funders Author Manuscripts

Europe PMC Funders Author Manuscripts

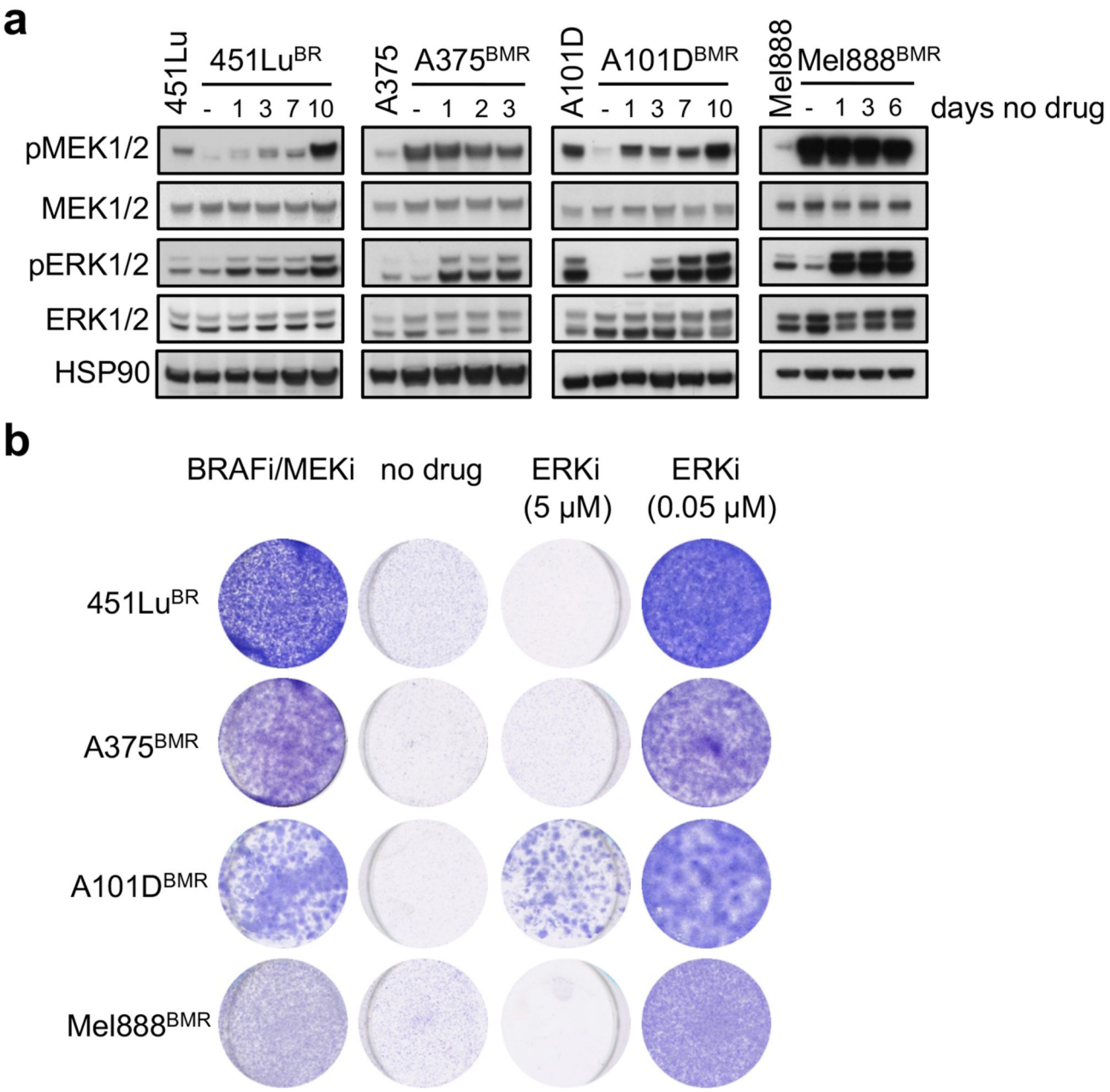

Extended Data Figure 4. ERK rebound contributes to drug holiday lethality irrespective of drug resistance mechanism

(**a**) Four parental sensitive cell lines were cultured without MAPK inhibitors and their drug-resistant counterparts were cultured either in the presence (-) or absence of MAPK inhibitors for the indicated number of days. Total cell lysates were subjected to immunoblotting with indicated antibodies. HSP90 served as a loading control.

(**b**) 451Lu^{BR} cells were cultured in the presence of either 1 μM BRAFi, a high concentration (5 μM) of ERKi, a low concentration (0.05 μM) of ERKi, or with vehicle control (no drug). A375^{BMR}, A101D^{BMR} and Mel888^{BMR} cells were cultured with either 0.5 μM BRAFi

Europe PMC Funders Author Manuscripts

+ 0.05 μM MEKi, 5 μM ERKi, 0.05 μM ERKi or with vehicle control (no drug). Cells were fixed, stained and photographed after 14 days.

For gel source images, see Supplementary Fig. 1. Data in **a** and **b**are representative of two independent biological experiments.

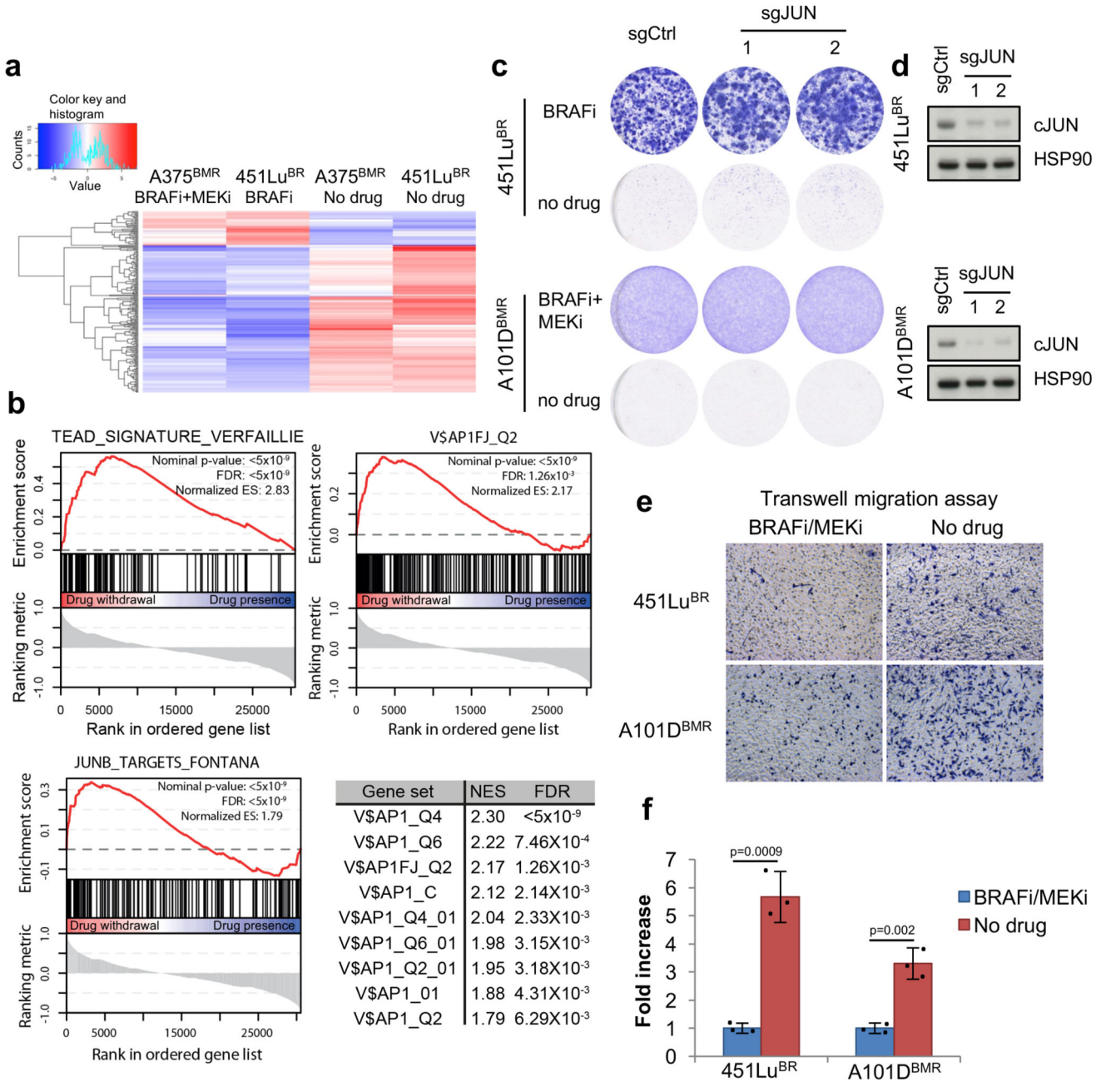

Extended Data Figure 5. Drug addiction is relayed by an MITF-dependent phenotype switch

(**a**) A375^{BMR} cells were cultured in the absence of 0.5 μM BRAFi + 0.05 μM MEKi for 0, 6, 24 and 48 hours and 451Lu^{BR} cells were cultured in the absence of 1 μM BRAFi for 0, 1, 3 and 5 days. Total RNA was isolated and subjected to sequencing analysis. Unsupervised

clustering of the 200 most variably expressed genes is represented for the first (0 hours / days) and last time points (48 hours / 5 days) in a heat map.

(**b**) Sequence data in (**a**; all time points) were subjected to gene set enrichment analysis to determine the correlation of the indicated gene sets with the drug addiction effect in $A375^{BMR}$ and $451Lu^{BR}$ cells. For p-value calculation, see Methods.

(**c**) $451Lu^{BR}$ and $A101D^{BMR}$ cells were infected with lentivirus encoding sgRNAs targeting genes encoding cJUN (sgJUN) or a scrambled sequence (sgCtrl). Cells were seeded in the presence or absence of MAPK inhibitors, and fixed, stained and photographed after 14 days (BRAFi or BRAFi+MEKi group) or 21 days (no drug group).

(**d**) Total cell lysates of the samples in (**c**) were subjected to immunoblotting analysis with indicated antibodies. HSP90 served as a loading control.

(**e**) $451Lu^{BR}$ and $A101D^{BMR}$ cells were cultured in the presence or absence of the MAPK inhibitors for 24 hours and then subjected to a transwell migration assay. The cells that migrated through the membrane were fixed, stained and photographed after 8 ($A101D^{BMR}$) or 24 ($451Lu^{BR}$) hours.

(**f**) Quantification of the migration capacity (**e**) from three representative images from each sample; P-value calculated by unpaired two-sided Student's t-test; Data in graphs are mean ± s.d.

For gel source images, see Supplementary Fig. 1. Data in **c, d** and **e** are representative of two independent biological experiments.

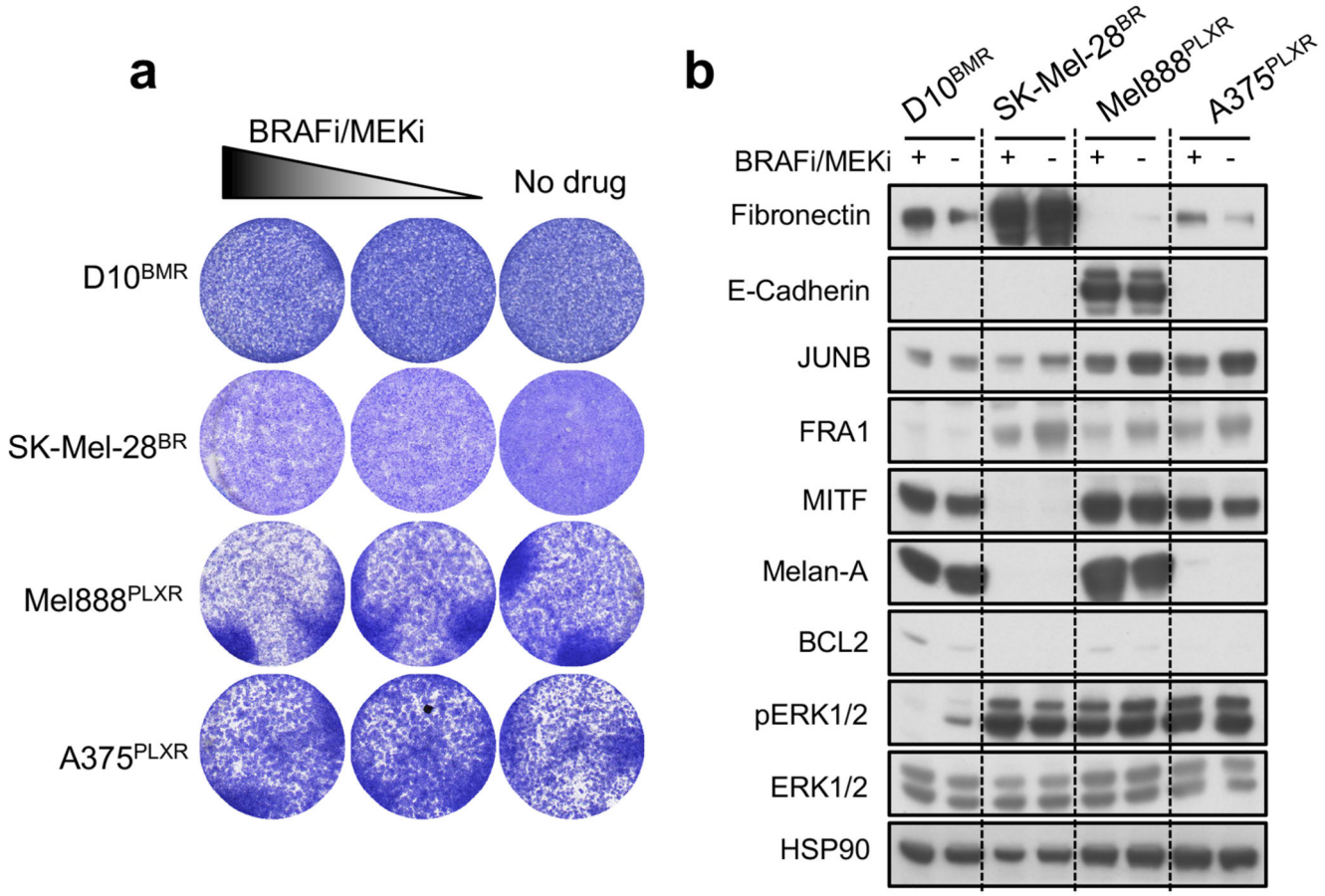

Extended Data Figure 6. Phenotype switch is not observed in non drug-addicted cells upon drug withdrawal

(**a**) D10^{BMR} cells were cultured with either 1 μM BRAFi + 0.1 μM MEKi, 0.5 μM BRAFi + 0.05 μM MEKi or with vehicle control (no drug); SK-Mel-28^{BR} were cultured with either 3 μM BRAFi dabrafenib, 1 μM dabrafenib or with vehicle control (no drug); Mel888^{PLXR} and A375^{PLXR} were cultured with either 3 μM BRAFi PLX4720, 1 μM PLX4720 or with vehicle control (no drug); Cells were fixed, stained and photographed after 10 days.

(**b**) Total cell lysates of the samples in (**a**) at day 3 were subjected to immunoblotting analysis with indicated antibodies. HSP90 served as a loading control.

For gel source images, see Supplementary Fig. 1. Data in **a** and **b** are representative of two independent biological experiments.

Europe PMC Funders Author Manuscripts

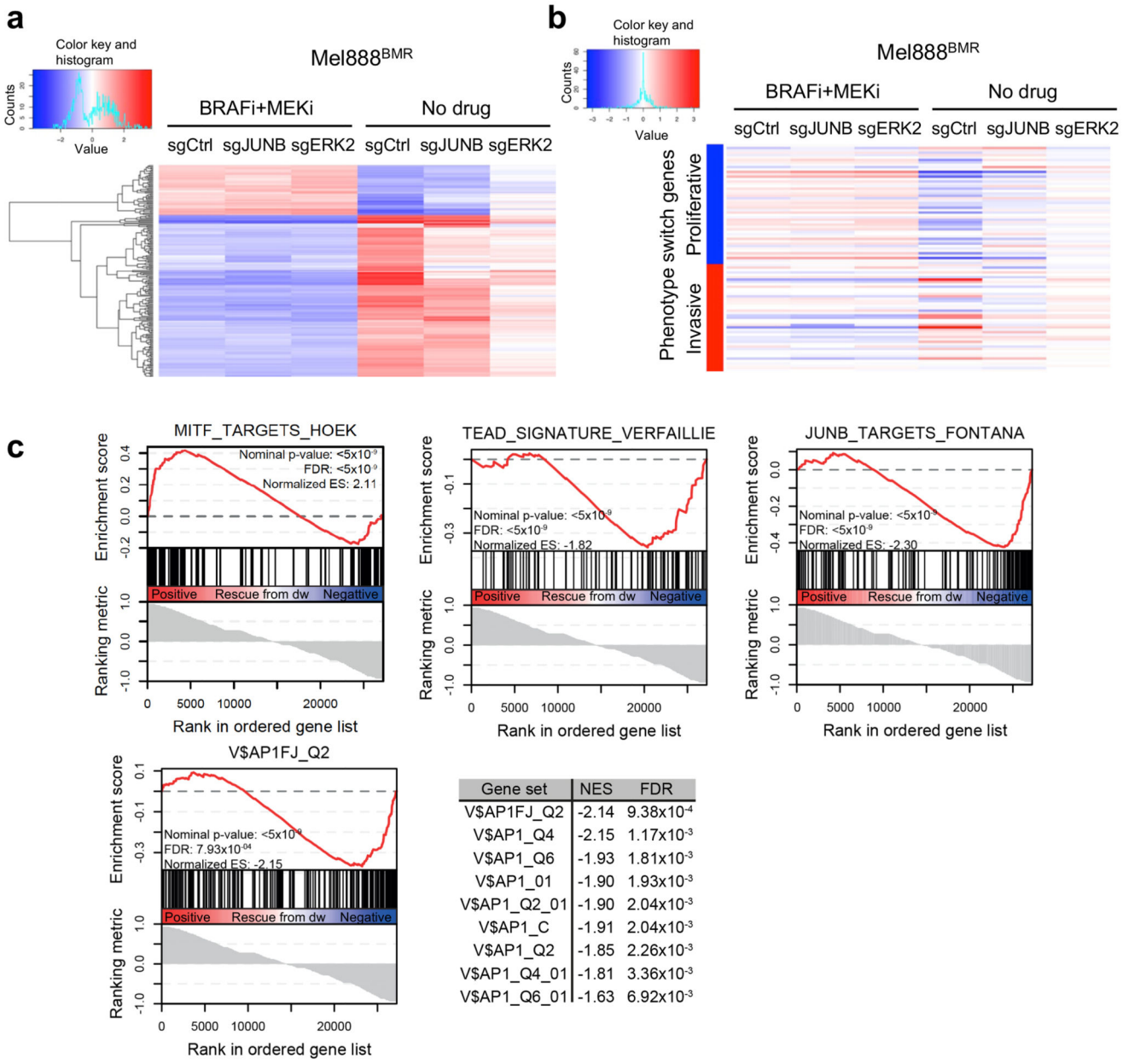

Gene set	NES	FDR
V$AP1FJ_Q2	-2.14	9.38×10^{-4}
V$AP1_Q4	-2.15	1.17×10^{-3}
V$AP1_Q6	-1.93	1.81×10^{-3}
V$AP1_01	-1.90	1.93×10^{-3}
V$AP1_Q2_01	-1.90	2.04×10^{-3}
V$AP1_C	-1.91	2.04×10^{-3}
V$AP1_Q2	-1.85	2.26×10^{-3}
V$AP1_Q4_01	-1.81	3.36×10^{-3}
V$AP1_Q6_01	-1.63	6.92×10^{-3}

Extended Data Figure 7. ERK2 and JUNB act in an MITF-dependent genetic phenotype switching program controlling drug addiction

(**a**) Mel888^{BMR} cells were infected with lentivirus harboring control scramble sgRNA (sgCtrl), JUNB sgRNA (sgJUNB) or ERK2 sgRNA (sgERK2). Cells were cultured in the presence or absence of 0.5 μM BRAFi + 0.05 μM MEKi for 5 days. Total RNA was isolated and subjected to sequencing analysis. Unsupervised clustering of the 200 most variably expressed genes are represented in a heat map.

(**b**) Genes involved in phenotype switching were selected from the sequence data in (**a**) and are represented in a heat map.

(**c**) Sequence data in (**a**) were subjected to gene set enrichment analysis to determine the correlation of the indicated gene sets with the extent of rescue of the drug addiction phenotype by sgJUNB and sgERK2 in Mel888^{BMR} cells. dw, drug withdrawal. For p-value calculation, see Methods.

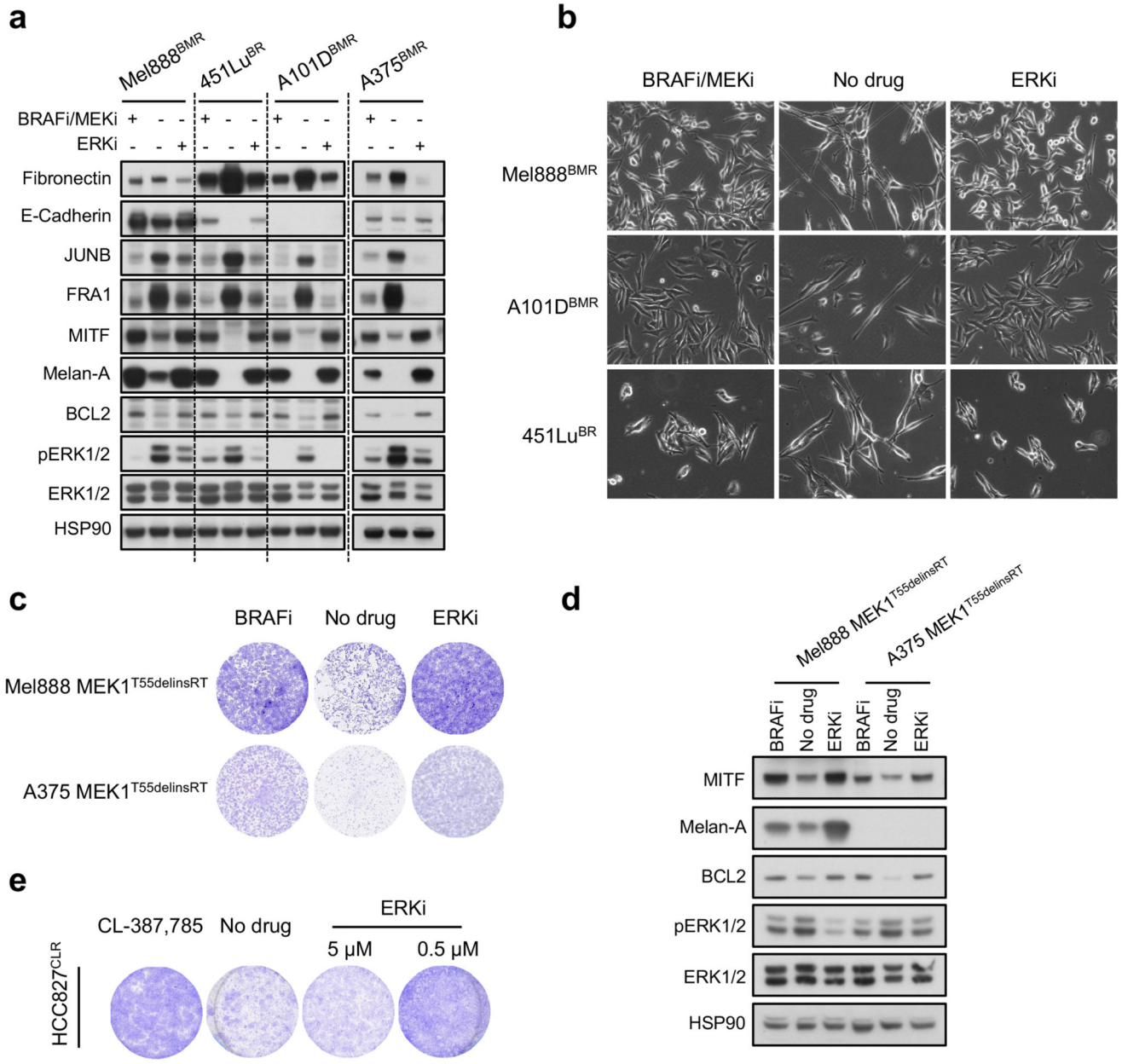

Extended Data Figure 8. Pharmacologic ERK inhibition blocks phenotype switch in drug-addicted cells upon drug withdrawal

(**a**) Mel888^{BMR}, A101D^{BMR} and A375^{BMR} cells were cultured with either 0.5 μM BRAFi + 0.05 μM MEKi, vehicle or 0.05 μM ERKi, 451Lu^{BR} cells were cultured with either 1 μM

Europe PMC Funders Author Manuscripts

BRAFi, vehicle or 0.05 μM ERKi for 3 days. Total cell lysates were subjected to immunoblotting with indicated antibodies. HSP90 served as a loading control.
(**b**) Photographs were taken from cells in (**a**) at day 3.
(**c**) Mel888 MEK1^{T55delinsRT} and A375 MEK1^{T55delinsRT} cells were culture in the presence of either 0.3 μM BRAFi, low concentration (0.05 μM) of ERKi or vehicle control (no drug). Cells were fixed, stained and photographed after 10 days.
(**d**) Total cell lysates from cells in (**c**) at day 5 were subjected to immunoblotting with indicated antibodies. HSP90 served as a loading control.
(**e**) HCC827^{CLR} cells were cultured in the presence of either 1 μM EGFR TKI CL-387,785, a high concentration (5 μM) of ERKi, a low concentration (0.5 μM) of ERKi, or with vehicle control (no drug). Cells were fixed, stained and photographed after 14 days.
For gel source images, see Supplementary Fig. 1. Data in **a**-**e** are representative of three independent biological experiments.

Europe PMC Funders Author Manuscripts

Europe PMC Funders Author Manuscripts

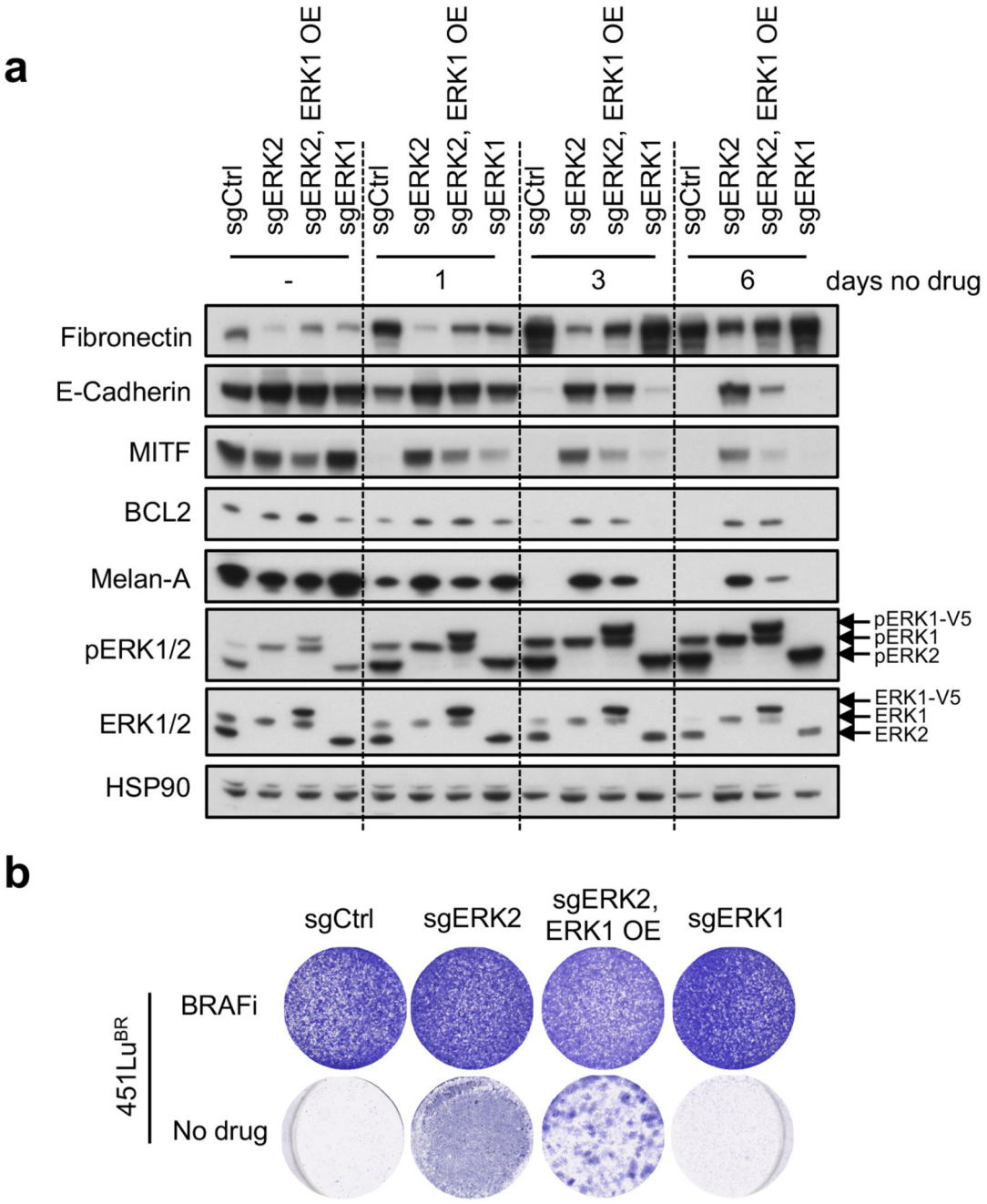

Extended Data Figure 9. ERK2 and ERK1 have distinct functions in drug addiction

(**a**) 451Lu^{BR} control cells (sgCtrl), ERK2 knockout cell (sgERK2), ERK1 (v5-tagged)-overexpressing sgERK2 cells (sgERK2, ERK1 OE) and ERK1 knockout cells (sgERK1) were cultured in the presence or absence of 1 μM BRAFi for up to 6 d. Total cell lysates were subjected to immunoblotting analysis with indicated antibodies. HSP90 served as a loading control.

(**b**) Cells described in (**a**) were cultured in the presence or absence of BRAFi, and fixed, stained and photographed after 14 days (BRAFi group) or 21 days (no drug group).

For gel source images, see Supplementary Fig. 1. Data in **a** and **b** are representative of two independent biological experiments.

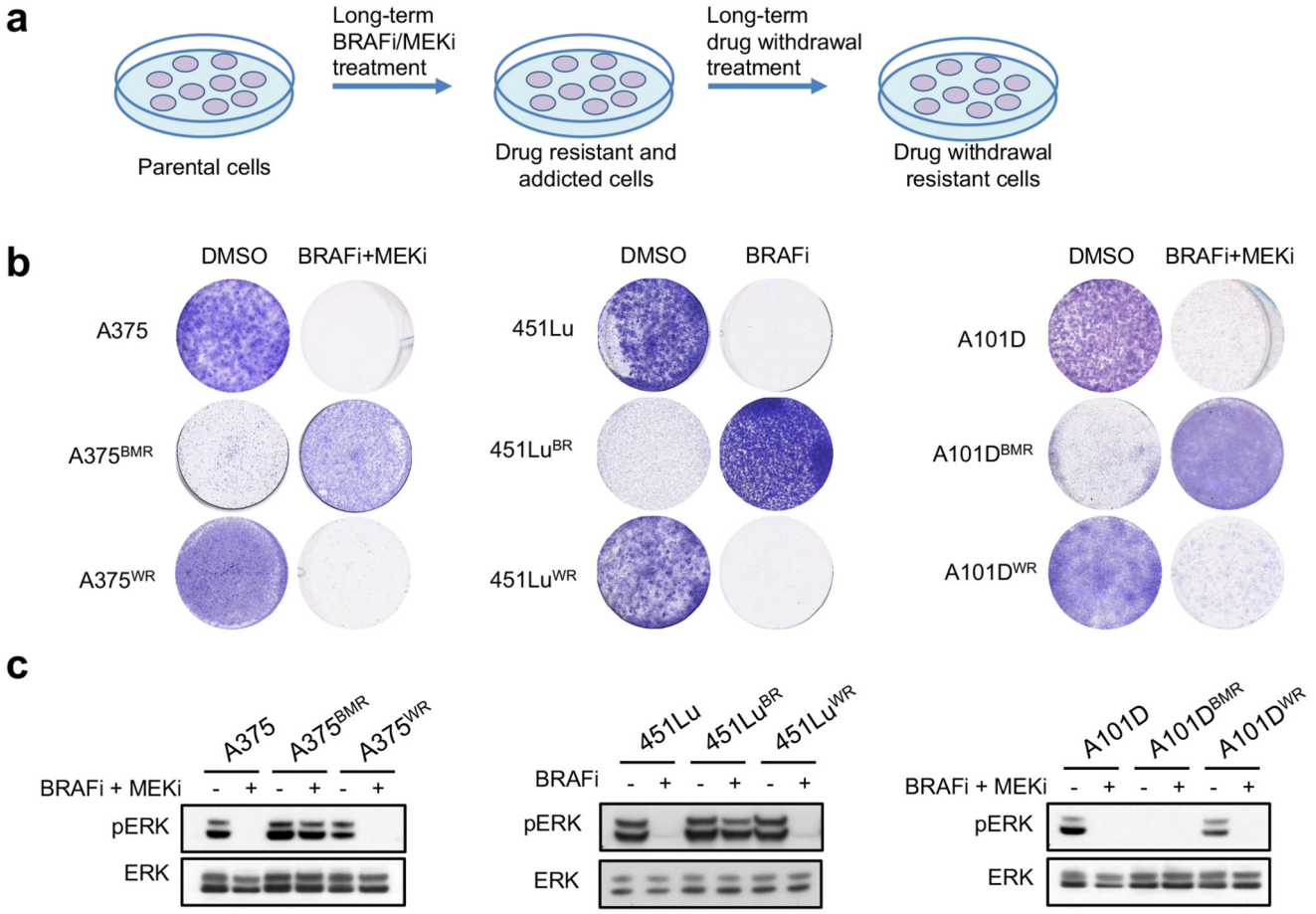

Extended Data Figure 10. Dynamic phenotype of drug resistance and drug addiction in melanoma

(**a**) Schematic flow chart indicating drug withdrawal resistant cells were generated from drug-addicted cells with long-term drug withdrawal.

(**b**) Parental (A375, 451Lu and A101D) cells, acquired drug resistant (A375^{BMR}, 451Lu^{BR} and A101D^{BMR}) and spontaneous developed drug withdrawal-resistant (A375^{WR}, 451Lu^{WR} and A101D^{WR}) cells were cultured with either MAPKi or vehicle. Cells were fixed, stained and photographed after 14 days.

(**c**) Total cell lysates from cells in (**b**) were subjected to immunoblotting with pERK and ERK antibodies after 6 hours of treatment.

For gel source images, see Supplementary Fig. 1. Data in **b** and **c** are representative of three independent biological experiments.

Supplementary Material

Refer to Web version on PubMed Central for supplementary material.

Acknowledgements

We are grateful to Kenichi Suda and Tetsuya Mitsudomi (Kindai University, Osaka-Sayama, Japan) for a gift of HCC827 and HCC827^{CLR} cells, Jessie Villanueva (The Wistar Institute, Philadelphia, USA) for 451Lu cells, Inge de Krijger (The Netherlands Cancer Institute) for technical advice on FISH, Annegien Broeks and the NKI Biobank for help and Alwin Huitema for providing DTIC. We like to thank all members of the Peeper and Blank labs for helpful advice. This work was financially supported by the European Research Council under the European Union's Seventh Framework Programme (FP7/2007-2013) / ERC synergy grant agreement n° 319661 COMBATCANCER (X.K., D.S.P.), and a Fellowship (T.K.), a Queen Wilhelmina Award (D.S.P.) and grant n° 10304 (X.K., D.S.P.), all from the Dutch Cancer Society / Koningin Wilhelmina Fonds.

References

1. Suda K, et al. Conversion from the "oncogene addiction" to ‘drug addiction’ by intensive inhibition of the EGFR and MET in lung cancer with activating EGFR mutation. Lung Cancer. 2012; 76:292–299. [PubMed: 22133747]
2. Sun C, et al. Reversible and adaptive resistance to BRAF(V600E) inhibition in melanoma. Nature. 2014; 508:118–122. [PubMed: 24670642]
3. Moriceau G, et al. Tunable-combinatorial mechanisms of acquired resistance limit the efficacy of BRAF/MEK cotargeting but result in melanoma drug addiction. Cancer Cell. 2015; 27:240–256. [PubMed: 25600339]
4. Thakur Das M, et al. Modelling vemurafenib resistance in melanoma reveals a strategy to forestall drug resistance. Nature. 2013; 494:251–255. [PubMed: 23302800]
5. Seifert H, et al. Prognostic markers and tumour growth kinetics in melanoma patients progressing on vemurafenib. Melanoma Res. 2016; 26:138–144. [PubMed: 26684061]
6. Dietrich S, et al. Continued response off treatment after BRAF inhibition in refractory hairy cell leukemia. J Clin Oncol. 2013; 31:e300–3. [PubMed: 23690412]
7. Dooley AJ, Gupta A, Middleton MR. Ongoing Response in BRAF V600E-Mutant Melanoma After Cessation of Intermittent Vemurafenib Therapy: A Case Report. Target Oncol. 2016; 11:557–563. [PubMed: 26857260]
8. Shalem O, et al. Genome-scale CRISPR-Cas9 knockout screening in human cells. Science. 2014; 343:84–87. [PubMed: 24336571]
9. Kemper K, et al. BRAF(V600E) Kinase Domain Duplication Identified in Therapy-Refractory Melanoma Patient-Derived Xenografts. Cell Reports. 2016; 16:263–277. [PubMed: 27320919]
10. Hoek KS, Goding CR. Cancer stem cells versus phenotype-switching in melanoma. Pigment Cell Melanoma Res. 2010; 23:746–759. [PubMed: 20726948]
11. Hoek KS, et al. In vivo switching of human melanoma cells between proliferative and invasive states. Cancer Res. 2008; 68:650–656. [PubMed: 18245463]
12. Wellbrock C, Arozarena I. Microphthalmia-associated transcription factor in melanoma development and MAP-kinase pathway targeted therapy. Pigment Cell Melanoma Res. 2015; 28:390–406. [PubMed: 25818589]
13. Garraway LA, et al. Integrative genomic analyses identify MITF as a lineage survival oncogene amplified in malignant melanoma. Nature. 2005; 436:117–122. [PubMed: 16001072]
14. Verfaillie A, et al. Decoding the regulatory landscape of melanoma reveals TEADS as regulators of the invasive cell state. Nature Communications. 2015; 6:6683.
15. Konieczkowski DJ, et al. A melanoma cell state distinction influences sensitivity to MAPK pathway inhibitors. Cancer Discov. 2014; 4:816–827. [PubMed: 24771846]
16. Müller J, et al. Low MITF/AXL ratio predicts early resistance to multiple targeted drugs in melanoma. Nature Communications. 2014; 5:5712.
17. The transcription cofactor c-JUN mediates phenotype switching and BRAF inhibitor resistance in melanoma. 2015; 8:ra82–ra82.
18. Riesenberg S, et al. MITF and c-Jun antagonism interconnects melanoma dedifferentiation with pro-inflammatory cytokine responsiveness and myeloid cell recruitment. Nature Communications. 2015; 6:8755.

19. Shin S, Dimitri CA, Yoon S-O, Dowdle W, Blenis J. ERK2 but not ERK1 induces epithelial-to-mesenchymal transformation via DEF motif-dependent signaling events. Molecular Cell. 2010; 38:114–127. [PubMed: 20385094]
20. Kemper K, et al. Intra- and inter-tumor heterogeneity in a vemurafenib-resistant melanoma patient and derived xenografts. EMBO Mol Med. 2015; 7:1104–1118. [PubMed: 26105199]
21. Seghers AC, Wilgenhof S, Lebbe C, Neyns B. Successful rechallenge in two patients with BRAF-V600-mutant melanoma who experienced previous progression during treatment with a selective BRAF inhibitor. Melanoma Res. 2012; 22:466–472. [PubMed: 22584957]
22. Schreuer M, et al. Combination of dabrafenib plus trametinib for BRAF and MEK inhibitor pretreated patients with advanced BRAF(V600)-mutant melanoma: an open-label, single arm, dual-centre, phase 2 clinical trial. The Lancet Oncology. 2017; 18:464–472. [PubMed: 28268064]
23. Harries M, et al. Treatment patterns of advanced malignant melanoma (stage III-IV) - A review of current standards in Europe. Eur J Cancer. 2016; 60:179–189. [PubMed: 27118416]
24. Jain T, Bryce A. Intermittent BRAF Inhibition Can Achieve Prolonged Disease Control in BRAF Mutant Melanoma. Cureus. 2015; 7:e410. [PubMed: 26824010]
25. Abdel-Wahab O, et al. Efficacy of intermittent combined RAF and MEK inhibition in a patient with concurrent BRAF- and NRAS-mutant malignancies. Cancer Discov. 2014; 4:538–545. [PubMed: 24589925]
26. Dooley AJ, Gupta A, Bhattacharyya M, Middleton MR. Intermittent dosing with vemurafenib in BRAF V600E-mutant melanoma: review of a case series. Ther Adv Med Oncol. 2014; 6:262–266. [PubMed: 25364391]
27. van Steensel B, Smogorzewska A, de Lange T. TRF2 protects human telomeres from end-to-end fusions. Cell. 1998; 92:401–413. [PubMed: 9476899]
28. Vredeveld LCW, et al. Abrogation of BRAFV600E-induced senescence by PI3K pathway activation contributes to melanomagenesis. Genes Dev. 2012; 26:1055–1069. [PubMed: 22549727]
29. Fontana MF, et al. JUNB is a key transcriptional modulator of macrophage activation. J Immunol. 2015; 194:177–186. [PubMed: 25472994]
30. Subramanian A, et al. Gene set enrichment analysis: a knowledge-based approach for interpreting genome-wide expression profiles. Proc Natl Acad Sci USA. 2005; 102:15545–15550. [PubMed: 16199517]

Europe PMC Funders Author Manuscripts

Europe PMC Funders Author Manuscripts

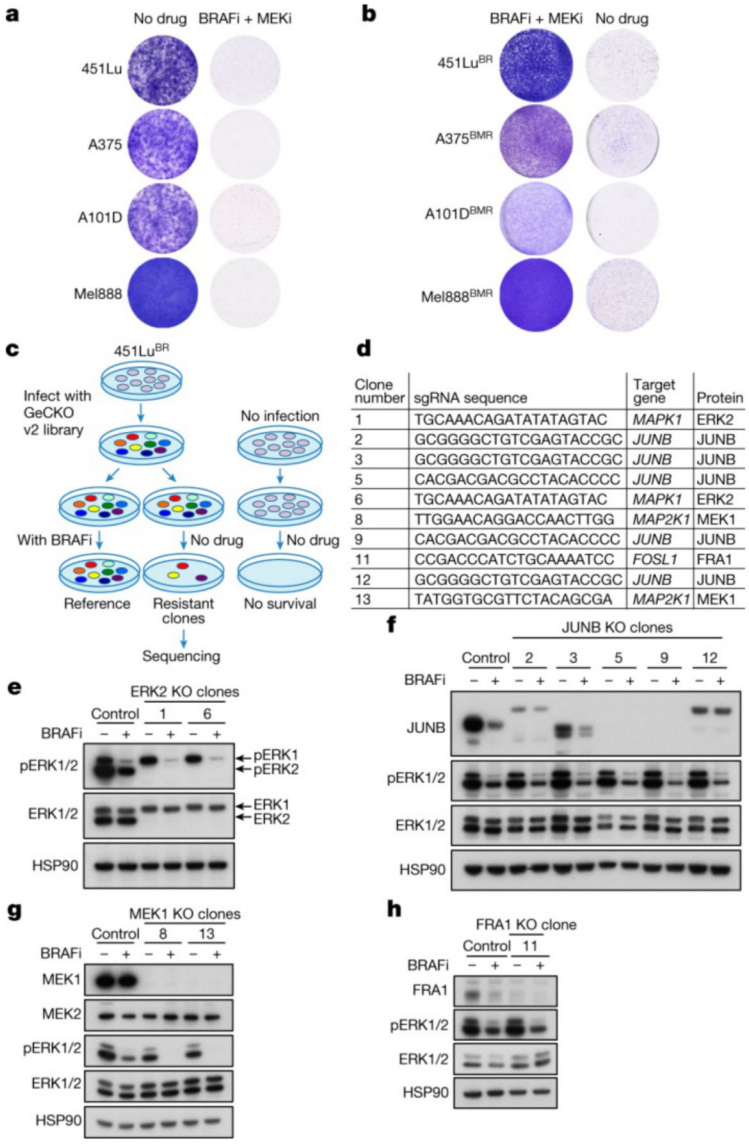

Figure 1. Genome-wide CRISPR-Cas9 knockout screen to break cancer drug addiction identifies several signaling pathway components

a, BRAF mutant melanoma cells treated with 1 μM dabrafenib (451Lu) or 0.5 μM dabrafenib + 0.05 μM trametinib (A375, A101D and Mel888) and stained 10 d later. **b,** BRAFi-resistant 451Lu^{BR} cells were cultured with or without 1 μM dabrafenib; BRAFi + MEKi-resistant A375^{BMR}, A101D^{BMR} and Mel888^{BMR} cells with or without 0.5 μM dabrafenib + 0.05 μM trametinib and stained after 2 (treated) or 3 wks (untreated). **c-d,** Screen outline and hits for which the same target gene was found in more than 2 independent screen clones. **e-h,** Control cells and screen clones as indicated, following dabrafenib or no treatment, were analyzed by immunoblotting. KO, knockout. For gel source images, see Supplementary Fig. 1. Data in a, b, e, f, g and h are representative of 3 independent biological experiments.

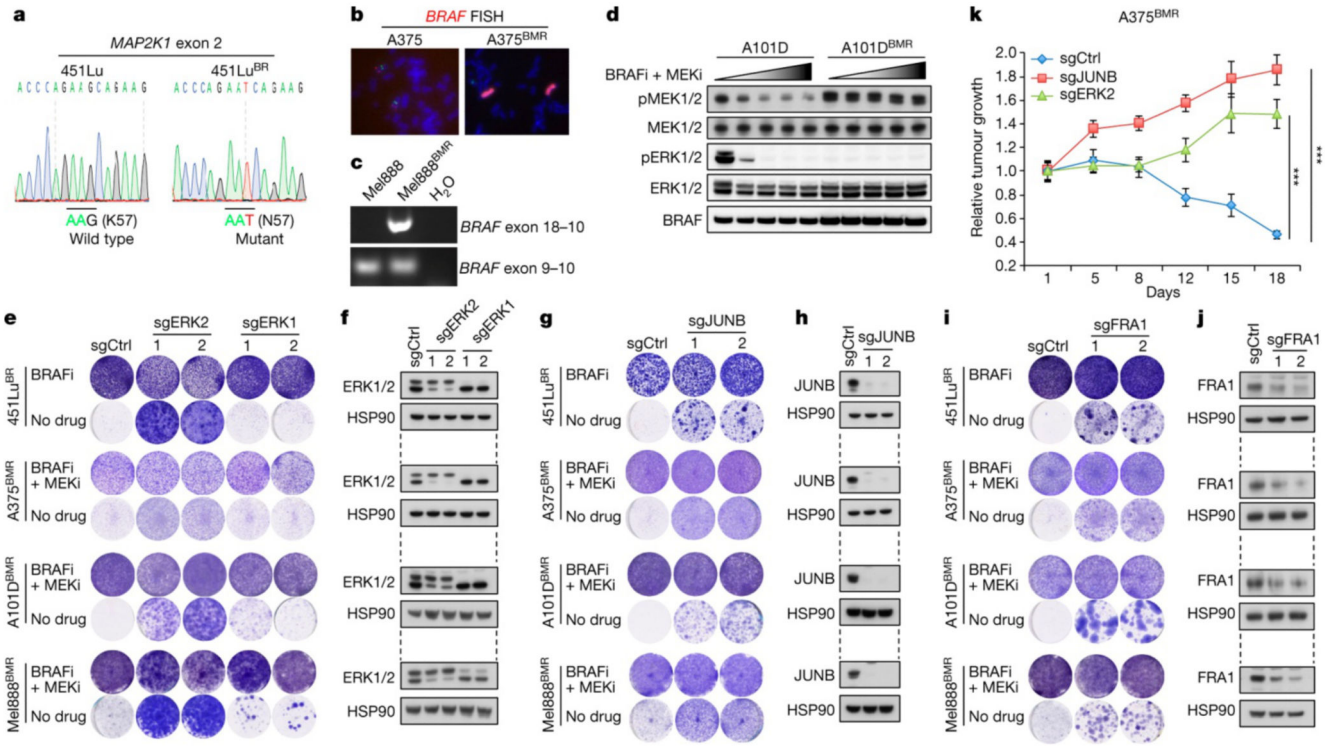

Figure 2. Conserved drug addiction pathway despite different therapy resistance mechanisms

a, *MEK1* exon 2 sequence of 451Lu and 451Lu^{BR} cells. **b,** Fluorescence In Situ Hybridization on metaphase spreads of A375 and A375^{BMR} cells using probes for *BRAF* (red) and a chromosome 7 centromeric region (green). **c,** RT-PCR on cDNA from Mel888 and Mel888^{BMR} cells using *BRAF* exon 18 forward and exon 10 reverse primers. A *BRAF* exon 9-10 amplification serves as a control. **d,** A101D and A101D^{BMR} cells were treated with increasing concentrations of dabrafenib + trametinib (0 + 0, 0.01 + 0.001, 0.1 + 0.01, 1 + 0.1 and 10 + 1 μM) and immunoblotted. **e-j,** A melanoma cell line panel was infected with lentivirus expressing sgRNAs targeting the indicated genes or a control sgRNA. Cells were cultured with or without drugs and stained (e, g, i) or immunoblotted (f, h, j). **k**, A375^{BMR} cells ablated for the indicated genes were s.c. injected into both flanks of immune-deficient NSG mice. Mice (n=5/group) received 30 mg/kg dabrafenib and 0.3 mg/kg trametinib from the first day of tumor injection onwards. After 7 days, treatment was discontinued for all mice. The graph represents fold change in tumor volume normalized on the volume on the day of treatment discontinuation. Data in graphs are mean ± s.e.m. ***, p<0.001 by unpaired two-sided Student's t-test. For tumor volume measurements, see Supplementary table 3. For gel source images, see Supplementary Fig. 1. Data in b-j are representative of three independent biological experiments.

Europe PMC Funders Author Manuscripts

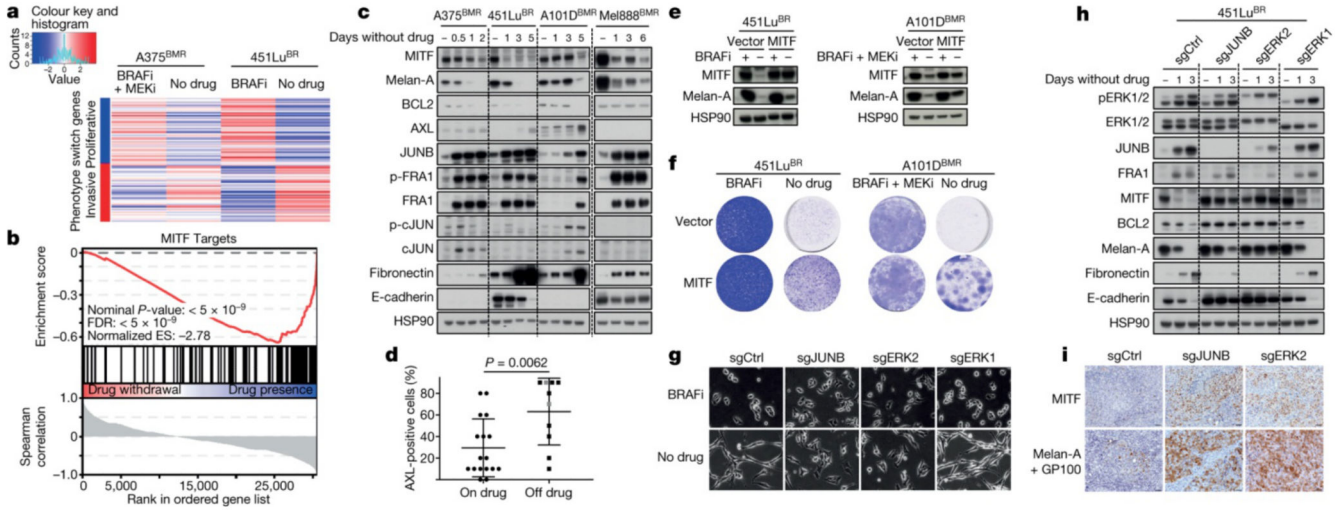

Figure 3. ERK2 and JUNB act in an MITF-dependent genetic phenotype switch controlling drug addiction

a, A375^{BMR} cells were cultured with or without 0.5 μM dabrafenib + 0.05 μM trametinib for 0, 6, 24 and 48 h, 451Lu^{BR} cells with or without 1 μM dabrafenib for 0, 1, 3 and 5 d, and analyzed for RNA expression. Phenotype switch genes were selected from the sequence data and the t_0 and the last time points are represented in a heat map. **b**, Sequence data from **a** (all time points) were subjected to Gene Set Enrichment Analysis. For p-value calculation, see Methods. **c**, Drug-addicted melanoma cell line panel was cultured with or without MAPK inhibitors for the indicated amount of time and immunoblotted. **d,** AXL immunostaining of a sample cohort of BRAFi-resistant patients on (n=17) or off (n=10) treatment. Samples in the "off drug" group were taken at a maximum of 3 months after drug discontinuation. Indicated in grey are 2 patients who had already received a first cycle of ipilimumab at the time of biopsy; the other patients did not receive any treatment at time of biopsy. Data in graphs are mean ± s.d.; P-value calculated by two-sided Mann–Whitney test; Confidence interval 95%. **e-f,** Cells expressing empty vector or MITF cDNA were cultured with or without inhibitors for 5 d and immunoblotted (**e**) or stained 2-3 wks later (**f**). **g-h**, 451Lu^{BR} cells ablated for the indicated genes were cultured with or without dabrafenib and photographed (**g**) or immunoblotted (**h**) 3d later. **i**, Tumors from **2k** were immunostained 18 d after drug discontinuation. Scale bar, 50 μm. For gel source images, see Supplementary Fig. 1. Data in c, e, f, g and h are representative of 3 independent biological experiments.

Europe PMC Funders Author Manuscripts

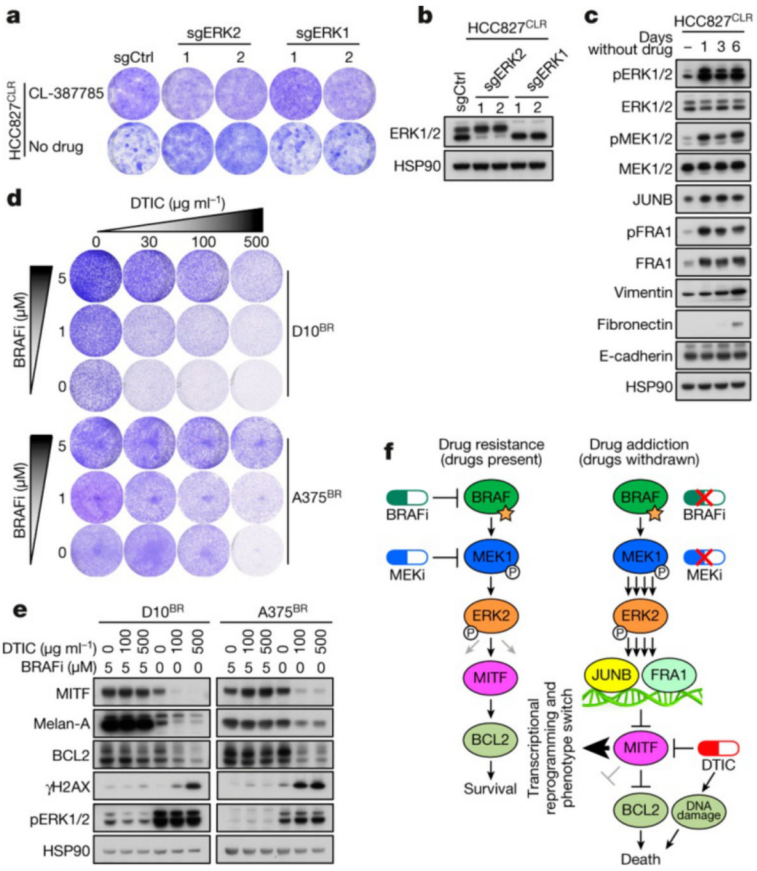

Figure 4. Conservation of drug addiction mechanism in human lung cancer cells and drug addiction synergizes with melanoma alkylating agent dacarbazine in tumor cell elimination

a-b, HCC827^{CLR} lung cancer cells ablated for the indicated genes were cultured with or without EGFR TKI CL-387,785 and stained 14 d later (**a**) or immunoblotted (**b**). **c**, HCC827^{CLR} cells were cultured with or without CL-387,785 for the indicated amount of time and immunoblotted. **d-e,** Moderately drug-addicted D10^{BR} and A375^{BR} melanoma cells were cultured in the presence of the indicated concentrations of dabrafenib and dacarbazine (DTIC) and stained 10 d later (**d**) or immunoblotted (**e**). For gel source images, see Supplementary Fig. 1. Data in a-e are representative of three independent biological experiments. **f**, Model for ERK2-dependent phenotype switch driving cancer drug addiction, in the context of drug pressure and resistance (left), and drug withdrawal causing addiction-associated lethality irrespective of drug resistance mechanism (right).

Europe PMC Funders Author Manuscripts